ARTICLE

Converting cytochrome *c* into a DyP-like metalloenzyme

Issei Omura[a], Koichiro Ishimori,[a,b] and Takeshi Uchida*[a,b]

Received 00th January 20xx,
Accepted 00th January 20xx

DOI: 10.1039/x0xx00000x

Dye-decolorizing peroxidase (DyP), which can degrade anthraquinone dyes using H_2O_2, is an attractive prospect for potential biotechnological applications for environmental purification. We previously designed an artificial DyP with an optimal pH for reactive blue 19 (RB19) degradation shifting from pH 4.5 to 6.5. We then attempted to degrade RB19 using *Escherichia coli* expressing this mutant, but RB19 was degraded equally compared with bacteria expressing wild-type (WT) DyP because most DyP was expressed in a heme-free form. In this study, we attempted to design an artificial peroxidase based on cytochrome *c* (cyt *c*), whose heme is covalently bound to the protein. We found that cyt *c* can degrade RB19, but its ability at pH 7.0 was ~60% of that of DyP from *Vibrio cholerae* at pH 4.5. To enhance this activity we constructed several mutants using three approaches. Initially, to improve reactivity with H_2O_2, Met80 was replaced with a noncoordinating residue, Ala or Val, but catalytic efficiency (k_{cat}/K_m) was increased by only ~1.5-fold. To enhance the substrate binding affinity we introduced an additional Trp by replacing Pro76 (P76W). The catalytic efficiency of this mutant was ~3-fold greater than that of WT cyt *c*. Finally, to form a hydrogen bond to axial histidine Gly29 was replaced with Asp (G29D). This mutant exhibited an ~80-fold greater dye-decolorizing activity. *Escherichia coli* expressing the G29D mutant was unable to degrade RB19 in solution due to degradation of heme itself, but this study provides new insights into the design of artificial DyPs.

Introduction

Dye-decolorizing peroxidase (DyP) (EC 1.11.1.19) is a member of the heme peroxidase family and has the ability to catalyze the oxidation of substrates using hydrogen peroxide (H_2O_2).[1] Typical substrates for DyPs are anthraquinone dyes, aromatic compounds that are difficult to degrade due to their complex and reinforced structures. As previously reported,[2–5] the dye-decolorizing reaction of DyPs does not occur in the heme pocket owing to the lack of space for bulky dye compounds near heme, in contrast with most heme enzymes whose reactions occur in the heme pocket as observed in P450 and horseradish peroxidase.[6,7] DyPs react with H_2O_2 and form compound I (Fe^{IV}=O porphyrin π-cation radical species) (Fig. S1A).[8] Recent studies have reported that the distal aspartic acid or arginine work as catalytic bases during the formation of compound I.[9,10] This radical is transferred then to Trp or Tyr on the protein surface, where the dye-decolorizing reaction occurs.[2–5] Therefore, DyPs have a broad substrate specificity, including not only small but also bulky compounds.

If industrial dyes are released into the environment, they remain in water and are harmful to living organisms. Thus, the dye degradation ability of DyPs is attractive for potential biotechnological applications for the treatment of water pollution. For biotechnological use, the stability of enzymes must be improved. Several studies have focused on improving the stability and reusability of enzymes by immobilizing them on mesoporous materials.[11–13] However, a decrease in enzymatic activity or inactivation is a potential risk of protein immobilization. To avoid this problem, a whole-cell biocatalyst is an attractive approach. This is a system employing *Escherichia coli*, in which enzymes are expressed. In this system, the natural cellular environment protects the enzymes from destabilization and deactivation.

In the case of DyPs, the pH dependence of the catalytic activity can be a problem when used in this system. The optimal pH of the dye-decolorizing reaction of DyPs is 3-4,[2,14] and its activity at neutral pH is less than 1/3,000 of the activity at acidic pHs. To solve this problem, we identified the decisive factor governing the low pH preference of DyP in *Vibrio cholerae* (*Vc*DyP) and constructed a mutant with improved dye-decolorizing activity at neutral pH. When Asp138, a residue present near heme, was replaced with Val, the optimal pH shifted from 4.5 to 6.5.[15] We attempted then to degrade reactive blue 19 (RB19) (Fig. S1B), a representative anthraquinone dye, using *E. coli*, where *Vc*DyP was overexpressed. The absorption of RB19 was reduced by almost half (Fig. S2). Degradation of RB19 in *E. coli* expressing the D138V mutant was greater than in *E. coli* expressing wild-type (WT) *Vc*DyP, but not as much as expected given the results of *in vitro* catalytic data. This was because *Vc*DyP in *E. coli* was mainly expressed in a heme-free form, which cannot react with H_2O_2. Thus, DyPs are not suitable for application to whole-cell biocatalysis.

In contrast to DyPs, the heme of cytochrome *c* (cyt *c*), a heme protein associated with electron transfer in the respiratory chain, is bound to the polypeptide through covalent bonds (Fig. S3).[16] Cyt *c* plays a major role in electron transfer in the respiratory chain, but can also function as peroxidase when Met80, one of the heme ligands, dissociates from the heme iron.[17,18] Several studies have reported that dissociation of Met80 from heme is caused by the interaction of cyt *c* with cardiolipins in the mitochondrial membrane,

[a] *Graduate School of Chemical Sciences and Engineering, Hokkaido University, Sapporo 060-8628, Japan*
[b] *Department of Chemistry, Faculty of Science, Hokkaido University, Sapporo 060-0810, Japan. E-mail: uchida@sci.hokudai.ac.jp*
† *Footnotes relating to the title and/or authors should appear here.*
Electronic Supplementary Information (ESI) available: [details of any supplementary information available should be included here]. See DOI: 10.1039/x0xx00000x

leading to a significant increase (> 50-fold) in peroxidase activity.[17] This increase is accounted for by the formation of pentacoordinated or hexacoordinated heme bound with a water, which increases the accessibility of H_2O_2 to the heme iron. However, it is unknown whether cyt *c* is capable of dye-degradation activity for anthraquinone dyes.

Recent studies have reported that rationally designed converted myoglobin (Mb) and neuroglobin, heme-containing proteins without dye-decolorizing activity, to be active species for dye decolorization.[19,20] In the case of Mb, introduction of Tyr at position 43 and Trp at position 138 in the heme pocket, with an additional Trp at position 88 on the protein surface, improved the dye-degrading activity by ~10-fold.[19] Tyr43 forms a cross-link with the heme 4-vinyl group to prevent heme dissociation upon unfolding,[21] and Trp138 contributes to tuning the structural rearrangement of myoglobin upon substrate binding.[22] Trp88 increases substrate binding affinity by ~2-fold. In this study, a similar strategy, introducing Trp near the putative binding site of RB19, was applied to cyt *c* to increase the reactivity of cyt *c* with the dye.

A structural feature of most DyPs is the proximal hydrogen bond between heme axial His and nearby Asp or Glu.[2,8,23] Mutation of Asp235 in cytochrome *c* peroxidase, which forms a hydrogen bond to the N_δ of the axial ligand His175 with Ala or Asn, abolished cyt *c* oxidative activity.[24] Applying this structural feature of peroxidases to cyt *c* could be expected to enhance the dye-degrading activity of cyt *c*. Thus, increasing pentacoordinate heme by replacing Met80 with a noncoordinating amino acid residue, introducing Trp on the protein surface, and forming a proximal hydrogen bond would likely create a functional enzyme for potential applications. Using these strategies, we found that the mutation of Gly29 to Asp led to the most prominent increase in catalytic efficiency compared with WT cyt *c*. Although the mutant did not work as a whole-cell biocatalyst, this study provides a new perspective for the structure-based design of artificial enzymes.

Results and Discussion

Dye-Decolorized Activity of Cyt *c*

We first measured the dye-decolorizing activity of cyt *c* at pH 7.0 using RB19 as a substrate. The activity was monitored using UV–visible absorption spectroscopy. The characteristic absorbance of RB19 at approximately 595 nm decreased after manual mixing of cyt *c* with H_2O_2 (20 mM) (Fig. 1A), and the blue solution turned colorless within 300 s. The result indicated that cyt *c* has dye-decolorizing activity. This result was unexpected because the tertiary structure and active site of cyt *c* are quite different from those of DyP (Fig. S4). To determine steady-state kinetic parameters (maximum rate, k_{cat} and Michaelis–Menten constant, K_m), the reactions were performed at a fixed concentration of RB19 (200 μM) at pH 7.0. The initial rates of RB19 degradation were obtained by fitting the decay of the absorption at 595 nm. The data were fitted to the Michaelis–Menten equation (Equation 1) (Fig. 1B), which provided $k_{cat,H2O2}$ of 5.6 ± 0.4 s^{-1} and $K_{m,H2O2}$ of 30 ± 4 mM.

We next monitored the dye-decolorizing activity of cyt *c* at a fixed concentration of H_2O_2 (20 mM). The initial rates were plotted against the concentrations of RB19 (Fig. 1C). Kinetic data exhibited a better

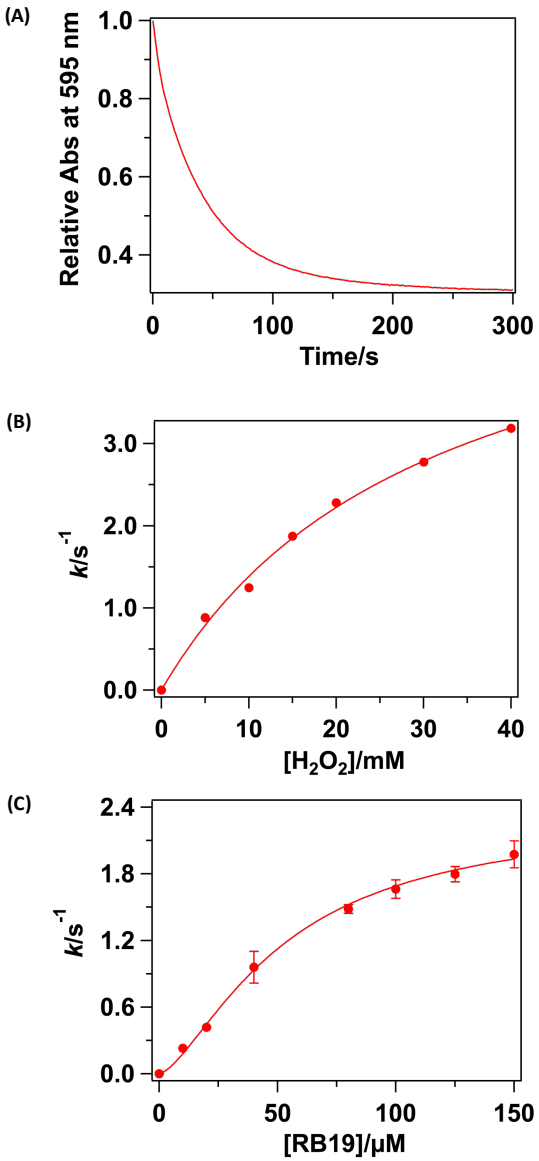

Fig. 1. Dye-decolorizing activity of WT cyt *c*. (A) Time-course of the dye-decolorizing reaction by WT cyt *c* at pH 7.0. The kinetic change of absorption at 595 nm during the reaction of cyt *c* (1.0 μM) and RB19 (40 μM) with H_2O_2 (20 mM) at 25 °C. (B) Initial rate ($k=v/[protein]$ in Equation 1) of RB19 (200 μM) oxidation at various concentrations (protein, 1.0 μM; pH 7.0). (C) Steady-state rates of oxidation as a function of RB19 concentration (0–150 μM) catalyzed by WT cyt *c* at pH 7.0.

fit to the Hill equation (Equation 2) than to the Michaelis–Menten equation. The evaluated $k_{cat,RB19}$ and $K_{m,RB19}$ values were 2.3 ± 0.1 s^{-1} and 53 ± 6 μM, respectively. The $k_{cat,RB19}$ value of cyt *c* was close to that of *Vc*DyP at the optimal pH, whereas the $K_{m,RB19}$ of cyt *c* was slightly greater than that of *Vc*DyP (Table 1). Therefore, the $k_{cat,RB19}/K_{m,RB19}$ of cyt *c* was 57% of that of *Vc*DyP.

Replacing the sixth axial ligand with a noncoordinating amino acid residue

As described above, we confirmed the dye-decolorizing activity of cyt *c*, which was comparable (~60%) to that of *Vc*DyP at pH 4.5 (Table 1). However, this assay was conducted at a relatively high concentration of H_2O_2 (20 mM). The turnover of the dye-decolorizing assay of cyt *c* at a low H_2O_2 concentration (200 μM H_2O_2) was calculated to be 0.7 min^{-1}, which was only ~2% of that of *Vc*DyP (36 min^{-1}). Thus, the dye-

Table 1: Kinetic parameters of WT cyt *c* and its mutants for RB19 decolorization

	RB19		
proteins	k_{cat} s^{-1}	K_m μM	k_{cat}/K_m s^{-1} mM^{-1}
WT	2.3 ± 0.1	53 ± 6	44 ± 6
M80A	2.4 ± 0.3	54 ± 13	45 ± 12
M80V	3.4 ± 0.1	49 ± 3	70 ± 5
P76W	3.4 ± 0.1	25 ± 2.0	138 ± 12
G29D	2.5 ± 0.1	0.70 ± 0.10	3625 ± 483
Y48H/M80A	1.5 ± 0.1	19 ± 4	77 ± 17
Y67H/M80A	2.6 ± 0.1	60 ± 3	44 ± 3
Y74H/M80A	2.5 ± 0.1	31 ± 3	80 ± 8
Y97H/M80A	1.8 ± 0.1	52 ± 6	34 ± 4
G41S	2.2 ± 0.1	19 ± 2	116 ± 13
Y48H	2.4 ± 0.2	38 ± 5	64 ± 10
A51V	2.6 ± 0.1	22 ± 2	117 ± 12
*Vc*DyP[a)]	2.3 ± 0.1	30 ± 3	77 ± 11
F43Y/F138W/P88W Mb[b)]	9.6 ± 0.2	8 ± 1	1200

[a]Reference 15, [b]Reference 19

decolorizing activity of cyt *c* requires higher concentrations of H_2O_2 than *Vc*DyP. Previous studies have shown that replacing the sixth axial ligand (Met80) of cyt *c* with Val increases the accessibility of H_2O_2 to heme, leading to enhancement (~10-fold) of peroxidase activity.[25,26] Accordingly, we expected that replacing Met80 with a noncoordinating amino acid, Ala (M80A) or Val (M80V), would increase the dye-decolorizing activity. The activity of the variants was evaluated by examining the initial rates of RB19 oxidation (Fig. 2A). Kinetic data show that the $k_{cat,RB19}$ values of the dye-decolorizing activities of the M80A and M80V mutants were 2.4 ± 0.3 s^{-1} and 3.4 ± 0.1 s^{-1}, respectively. The $K_{m,RB19}$ values of these mutants were 54 ± 13 μM and 49 ± 3 μM, respectively (Table 1). The k_{cat} of the M80V mutant was slightly greater than that of the WT (2.3 ± 0.1 s^{-1}), and the K_m was similar to that of the WT (53 ± 6 μM), leading to an ~1.5-fold increase in catalytic efficiency ($k_{cat,RB19}/K_{m,RB19}$). Although we expected that the substitution of Met80 would significantly improve the dye-degradation activity of cyt *c*, it did not.

To confirm whether the reactivity of heme with H_2O_2 was enhanced by the mutation of Met80 as expected, the steady-state kinetics of the M80A and M80V mutants were studied using a typical peroxidase substrate, guaiacol (Fig. S1C). The kinetic data at pH 7.0 (Fig. 2B) show that the $k_{cat,guaiacol}$ of peroxidase activities of the M80A and M80V mutants were 1.22 ± 0.04 and 2.6 ± 0.1 s^{-1}, respectively, 13- and 27-fold larger than that of WT cyt *c*, respectively. The $K_{m,guaiacol}$ values of the M80A and M80V mutants were 5.6 ± 0.9 and 2.9 ± 0.4 μM, almost the same (M80A) and half (M80 V) that of WT

Table 2. Kinetic parameters of WT cyt *c* and its mutants for guaiacol oxidation

	guaiacol		
proteins	k_{cat} s^{-1}	K_m μM	k_{cat}/K_m s^{-1} mM^{-1}
WT	0.096 ± 0.003	5.9 ± 0.8	16 ± 2
M80A	1.22 ± 0.04	5.6 ± 0.9	218 ± 36
M80V	2.6 ± 0.1	2.9 ± 0.4	896 ± 13
P76W	0.085 ± 0.001	8.3 ± 0.5	10 ± 1
G29D	1.57 ± 0.03	0.9 ± 0.1	1777 ± 203
native HRP[c)]	420 ± 40	5800 ± 700	72

[c]Reference[25]

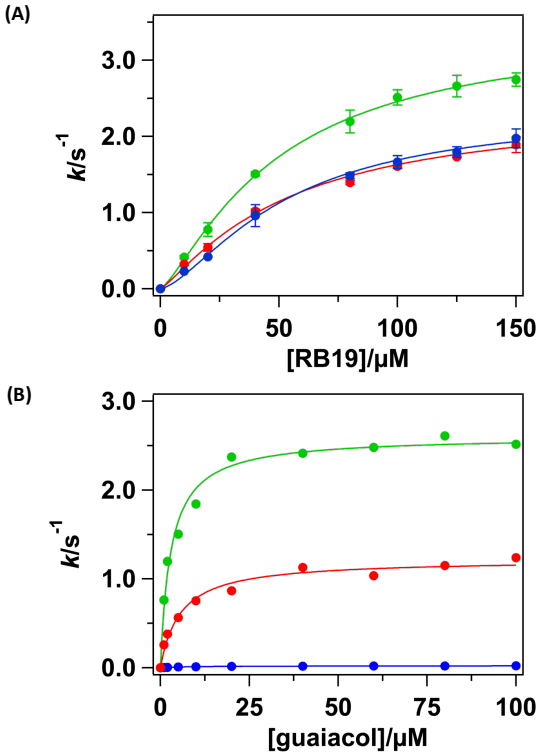

Fig. 2. Kinetic analysis of the H_2O_2-dependent reaction of WT (blue), M80A (red), and M80V (green). (A) Initial rates ($k=v/[protein]$) of oxidation as a function of RB19 concentration (0-150 μM) by proteins (protein, 1.0 μM; H_2O_2, 20 mM; pH 7.0). (B) Initial rates of oxidation as a function of guaiacol concentration (0-100 μM) catalyzed by proteins at pH 7.0(WT, 1.0 μM; M80A and M80V, 0.1 μM; H2O2, 10 mM; pH 7.0).

cyt *c*, respectively. The $k_{cat,guaiacol}/K_{m,guaiacol}$ values of the two variants were ~14–56-fold greater than those of WT cyt *c*. The values of the M80A and M80V mutants were ~3- and ~12-fold greater than those of native HRP[27] (Table 2), indicating that both mutants are good peroxidases. Considering that the peroxidase activity ($k_{cat,guaiacol}/K_{m,guaiacol}$) of the mutants was ~14–56-fold greater than that of WT cyt *c*, whereas their dye-degrading activity ($k_{cat,RB19}/K_{m,RB19}$) was less than 2-fold greater than that of WT cyt *c*, elimination of Met80 was effective in enhancing peroxidase activity, but did not contribute to the enhancement of dye-decolorizing activity. The $K_{m,RB19}$ value of the Met80 mutants was comparable to WT cyt *c*, suggesting that the radicals, which are formed at heme more rapidly by the mutation of Met80, are not efficiently transferred to the active site, or radicals that migrate to the active site are not well utilized for dye degradation.

Replacement of surface tyrosine with histidine

According to previous studies, the active site of the dye-decolorizing reaction of DyPs is Tyr or Trp at the protein surface,[2–5] to which radicals formed at heme transfer. In the case of *Vc*DyP, Tyr129 and Tyr235 are the putative active sites of the dye-decolorizing reaction[2]. cyt *c* has four Tyr residues (Tyr48, Tyr67, Tyr74, and Tyr97), all of which are located on the protein surface (Fig. 3), and has one Trp residue (Trp59) that is buried inside the protein. Therefore, we supposed that radicals generated by the reaction of heme with H_2O_2 are transferred to one or some of these four tyrosine residues. To determine the active site of dye degradation by cyt *c*, we prepared four Tyr mutants (Y48H/M80A, Y67H/M80A, Y74H/M80A, and Y97H/M80A), in which each Tyr and Met80 were replaced with His

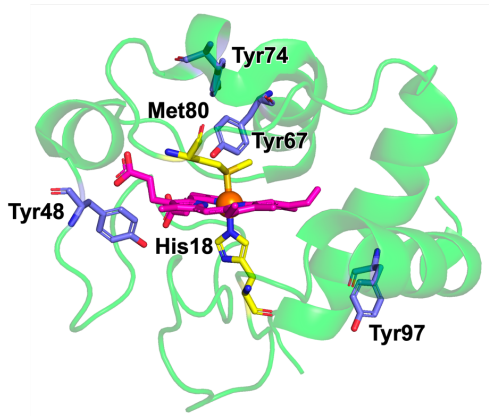

Fig. 3. Location of Tyr48, Tyr67, Tyr74 and Tyr97 in cyt *c* (PDB 6K9I).

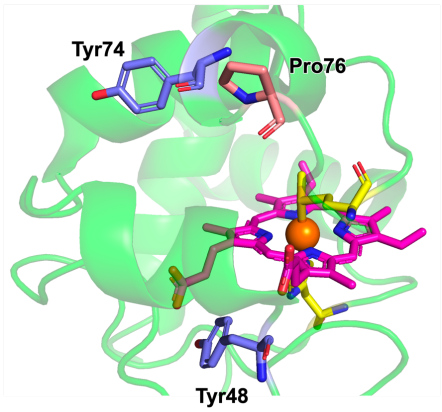

Fig. 5. Location of Tyr48, Tyr74 and Pro76 in cyt *c*.

and Ala, respectively, and evaluated their dye-decolorizing activity. Kinetic data analysis provided $k_{cat,RB19}$ for these mutants' dye-decolorizing activity of 1.5 ± 0.1 (Y48H/M80A), 2.6 ± 0.1 (Y67H/M80A), 2.5 ± 0.1 (Y74H/M80A) and 1.8 ± 0.1 s^{-1} (Y97H/M80A) (Table 1). The $K_{m,RB19}$ values of these mutants were 19 ± 4 (Y48H/M80A), 60 ± 3 (Y67H/M80A), 31 ± 3 (Y74H/M80A), and 52 ± 6 μM (Y97H/M80A) (Table 1). The $k_{cat,RB19}$ of these mutants was not much greater than that of WT cyt *c*, whereas the $K_{m,RB19}$ of the Y48H/M80A and Y74H/M80A mutants was ~1/3 and ~1/2 of that of WT, respectively. A more prominent feature of the Y48H/M80A and Y74H/M80A mutants is the presence of a lag phase at <20 mM H_2O_2 (Fig. 4). In the kinetic characterization of DyP from *Streptomyces lividans,* the presence of a lag-phase at low RB19 concentrations suggests that the rate-limiting step of the dye-decolorizing reaction is disproportion between dye radicals.[28] The presence of a lag phase for the Y48H/M80A and Y74H/M80A mutants suggests that this disproportionate rate would be decelerated by replacement of Tyr48 or Tyr74 with His, leading to a change in the rate-limiting step in these two mutants. Therefore, Tyr48 and Tyr74 are putative active sites for the dye-decolorizing reaction.

Dye-decolorizing activity of P76W cyt *c* derivatives

Since Tyr48 and/or Tyr74 were suggested to be the active sites, we attempted to increase the affinity of the substrate by introducing a hydrophobic residue near these residues. From the crystal structure of cyt *c*,[29] Pro76 is located between Tyr48 and Tyr74 and its side chain is exposed to the solvent (Fig. 5). Therefore, we constructed a mutant in which Pro76 was replaced with Trp (P76W) and measured dye-decolorizing activity. The obtained rate constants were plotted against the substrate concentration and fit to the Hill equation (Fig. 6). The $k_{cat,RB19}$ was 3.4 ± 0.1 s^{-1}, slightly greater than that of WT (2.3 s^{-1}), whereas the $K_{m,RB19}$ of the P76W mutant cyt *c* was 25 ± 2 μM, approximately half that of WT (53 μM) (Table 1). As a result, the $k_{cat,RB19}/K_{m,RB19}$ value for the P76W mutant was 138 s^{-1} mM^{-1}, ~3-fold greater than that of WT cyt *c* (44 s^{-1} mM^{-1}) (Table 1).

As described above, the $K_{m,RB19}$ of the P76W mutant was reduced to approximately half that of WT cyt *c*, as expected (Table 1). In a study of myoglobin mutants, the F43Y/F138W mutant with an additional introduction of Trp88 to the protein surface (F43Y/F138W/P88W), resulted in a ~10-fold smaller $K_{m,RB19}$ than that of WT Mb.[19] The results of docking simulations of this mutant with RB19 showed that the indole ring of Trp88 and the anthracene ring of RB19 adopted almost parallel structures, indicating a π-π stacking interaction.[19] The kinetics data of the P76W, mutant cyt *c* suggest that the substrate affinity of the mutant was increased by the hydrophobic interaction between RB19 and Trp76 but was not as pronounced as that of the F43Y/F138W/P88W mutant.

Cyt *c* contains three Ω-loop region: distal (residues 71–85), central (residues 40–57), and proximal (residues 12–39) Ω-loops.[29,30] The flexibility of the loops affects the structure of the heme pocket.[31] Pro76 is located in the 71-85 Ω-loop. Previous studies have reported

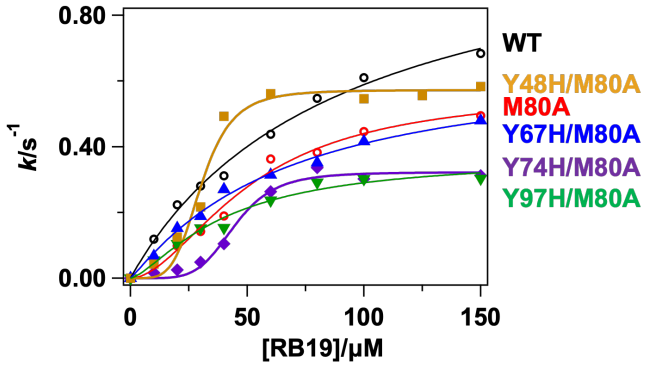

Fig. 4. Kinetic analysis of the H_2O_2-dependent reaction of WT (black), M80A (red), Y48H/M80A (ocher), Y67H/M80A (blue), Y74H/M80A (purple) and Y97H/M80A (green). Initial rates (k=v/[protein]) of oxidation as a function of RB19 concentration (0–150 μM) with H_2O_2 (10 mM) catalyzed by proteins at pH 7.0.

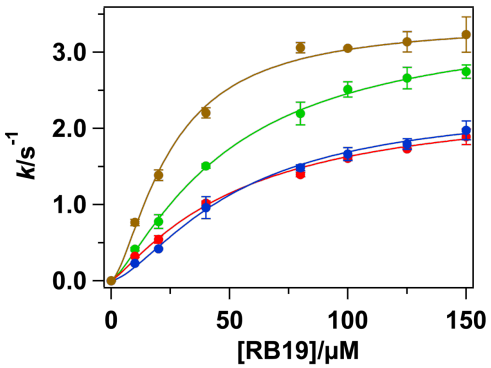

Fig. 6. Kinetic analysis of the H_2O_2-dependent reaction of WT (blue), M80A (red), M80V (blue), and P76W (lower). Kinetics of oxidation as a function of RB19 concentration (0–150 μM) with H_2O_2 (20 mM) catalyzed by proteins at pH 7.0.

that a yeast iso-1-cyt *c* mutant whose Phe82 was replaced with Gly had a 10-fold greater ability to oxidize polycyclic aromatic hydrocarbons compared to the WT yeast iso-1-cyt *c*[32] and increased the azide binding rate by ~6-fold.[33] Recent studies on human cyt *c* showed that the $k_{cat,guaiacol}$ of the mutant of Ile81 in the loop with Ala (I81A) was ~10-fold greater than that of WT cyt *c*,[34] and $k_{cat,ABTS}$ of Pro76 with Cys (P76C) was 13-fold greater than that of WT cyt *c*.[35] These data suggest that mutation of amino acid residues in the 71-85 Ω-loop destabilizes the coordination of Met80, which contributes to the increased peroxidase activity. However, the $k_{cat,guaiacol}/K_{m,guaiacol}$ value of the P76W mutant was 10 s^{-1} mM^{-1}, 60% that of the WT (Table 2). As a result, introduction of Trp near the putative active site for RB19 did not contribute as much as expected to improvement in the mutant's catalytic efficiency.

Dye-decolorizing activity of G41S, Y48H, and A51V variants

Replacing Pro76 with Trp enhanced dye-degrading activity by ~3-fold, but did not improve the reactivity with H_2O_2, which was less than those of mutants in the 71-85 Ω-loop such as P76C, I81A and F82G. Thus, we next focused on another Ω-loop of cyt *c*. Structural changes in the 40-57 Ω-loop have been reported to alter the accessibility of H_2O to heme.[35] Gly41, Tyr48, and Ala51 residues located in the 40-57 Ω-loop of cyt *c* (Fig. 7) were replaced with Ser, His, and Val, respectively, which led to increases in catalytic activity by ~7-fold.[36,37] We prepared the same cyt *c* mutants and measured their dye-decolorizing activity. Kinetic data show that the k_{cat} values for dye-decolorizing activity in the G41S, Y48H, and A51V mutants are 2.2 ± 0.1, 2.4 ± 0.2, and 2.6 ± 0.1 s^{-1}, respectively (Table 1). The K_m values were 19 ± 2 (G41S), 38 ± 5 (Y48H), and 22 ± 2 (A51V) μM. As a result, the G41S and A51V mutants exhibited a catalytic efficiency that was ~2.5-fold greater than that of the WT (Table 1). Previous studies reported that the G41S, Y48H, and A51V mutants have peroxidase activity ~7-fold greater than that of the WT human cyt *c* because of an increased population for the pentacoordinate heme species state.[36–38] However, the kinetic data from the G41S, Y48H, and A51V mutants suggest that the mutation of amino acid residues in the 40-57 Ω-loop led to a moderate improvement in dye-decolorizing activity.

Introduction of the proximal hydrogen bond

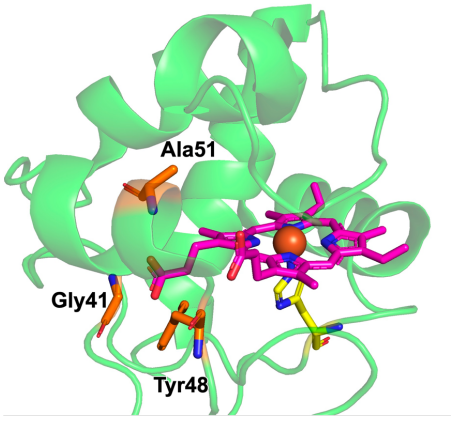

Fig.7. Location of Gly41, Tyr48 and Ala51 in cyt *c*.

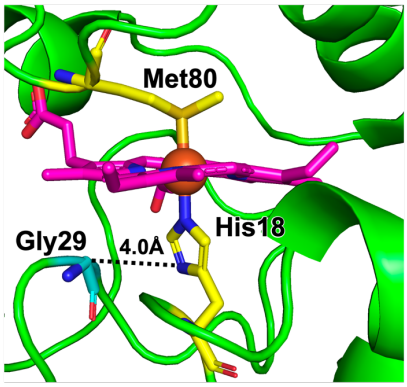

Fig.8. Location of His18 and Gly29 in cyt *c*. The distance between His18 and Gly29 is represented by the dotted line.

In most heme peroxidases the proximal His forms a hydrogen bond with nearby Asp or Glu.[39] This hydrogen bond imparts more imidazolate character to the His ligand, increasing its electron donating ability and facilitating the formation of the compound I intermediate. To promote the generation of radicals to improve dye degradation activity, we introduced the proximal hydrogen bond into cyt *c*. On the basis of the crystal structure of cyt *c* (PDB code: 6K9I), Gly29 is located ~4 Å from the proximal His (the distance between C_α of Gly29 and N_δ of His18 is 4.0 Å), and we constructed a mutant of Gly29 to Asp (G29D), which is presumed to be within hydrogen bond distance of the proximal His (Fig. 8). The absorption spectrum of the supernatant of the lysate of *E. coli* expressing WT cyt *c* has a split Q-band, characteristic of ferrous heme, whereas that of the G29D mutant did not, indicating conversion to the ferric form (Fig. S5A). The data suggest that the purified G29D mutant was easily oxidized, indicating the formation of a hydrogen bond between Asp29 and proximal His.

To confirm the effect of the introduced hydrogen bond, we measured the dye-decolorizing activity of the G29D mutant (Fig. 9A). As shown in Table 1, the G29D mutant exhibited almost the same $k_{cat,RB19}$ value and dramatically decreased $K_{m,RB19}$ compared to those of WT cyt *c*, resulting in ~80-fold higher overall catalytic efficiency ($k_{cat,RB19}/K_{m,RB19}$). The peroxidase activity of the mutant was also monitored using guaiacol under steady state conditions. The obtained rate constants were plotted against the substrate concentrations, and the plots were fit to the Michaelis–Menten equation (Fig. 9B). $k_{cat,guaiacol}$ and $K_{m,guaiacol}$ were 1.57 ± 0.03 s^{-1} and 0.9 ± 0.1 μM, respectively (Table 2). As a result, the mutant exhibited a significantly greater catalytic efficiency ($k_{cat,guaiacol}/K_{m,guaiacol}$) of 1777 ± 203 s^{-1} mM^{-1}, ~110-fold greater than that of WT cyt *c*.

The G29D mutant, which mimics the structural features of heme peroxidases, dramatically enhanced $k_{cat,RB19}/K_{m,RB19}$ (Table 1) and $k_{cat,guaiacol}/K_{m,guaiacol}$ (Table 2). However, the enhancement of the catalytic efficiency of dye decolorization is mainly attributed to $K_{m,RB19}$ but not $k_{cat,RB19}$ (Table 1). Gly29 is located in the 12-39 Ω-loop structure. The protein structure and peroxidase activity of the heme-proximal mutant of human cyt *c*, in which Thr28, a phosphorylation site, was replaced with Asp (T28D) or Glu (T28E), have been reported.[40,41] Both the T28D and T28E mutants exhibited peroxidase activity approximately twice that of WT cyt *c*. These results suggest that the introduction of the negative charge near the proximal heme may cause structural changes around heme. The introduction of a

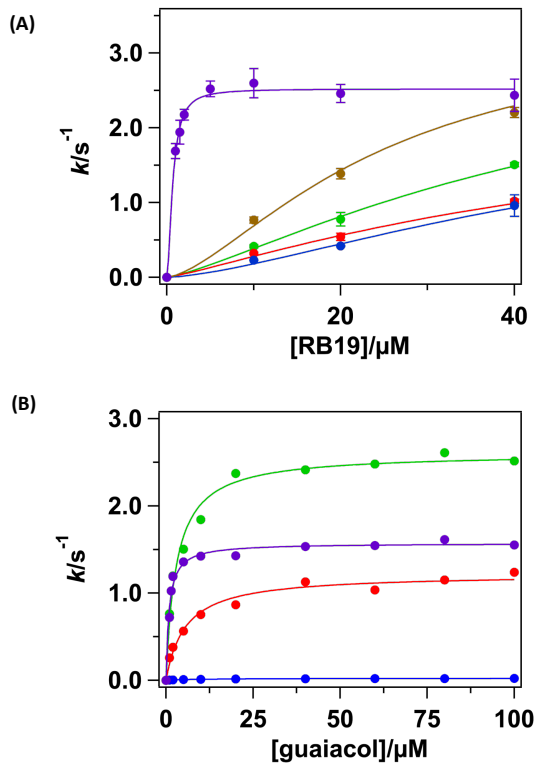

Fig. 9. Kinetic analysis of the H_2O_2-dependent reaction of WT (blue), M80A (red), M80V (blue), P76W (ocher), and G29D (purple). (A) Initial rates (k=v/[protein]) of oxidation as a function of RB19 concentration (0–40 μM) catalyzed by proteins at pH 7.0. (B) Initial rates of oxidation as a function of guaiacol concentration (0–100 μM) catalyzed by proteins at pH 7.0.

negative charge at the Gly29 position, which is closer to heme, caused a structural change that led to improved reactivity with substrates near heme. This idea may be supported by the CD spectra (Fig. S5B). The CD spectrum of the G29D mutant exhibited two negative bands at 208 and 222 nm (Fig. S4B). For a globular α-helical protein such as cyt *c*, perturbations of the $\theta_{222nm}/\theta_{208nm}$ ratio can be associated with changes in interhelical interactions resulting from changes to the packing of Trp side chains within a protein core.[42] For the G29D mutant, the $\theta_{222nm}/\theta_{208nm}$ ratio is 1.0, smaller than 1.3 as determined for WT cyt *c*. Therefore, it is postulated that the environment around heme was perturbed and flexibility was enhanced by replacing Gly29 with Asp. Moreover, the $K_{m,RB19}$ of the G29D mutant was greatly reduced compared to that of the WT (Table 1). The structural change around heme may also increase its accessibility to bulky substrates such as RB19.

Whole-cell biocatalyst using the G29D mutant cyt *c*

Finally, the G29D mutant was used as a whole-cell catalyst. The mutant was expressed in the periplasmic space, where substrates are more easily accessible than in the cytoplasm. Coexpression with cytochrome c maturation proteins helps cyt *c* form covalent bonds (thioether bonds) with heme. A reddish *E. coli* pellet indicates the expression of the G29D mutant as a heme-bound form. The decolorizing abilities of *E. coli* were monitored as the decrease in the absorbance at 595 nm over time. The absorption spectrum of the culture medium containing RB19 changed little after 24 hours and thus *E. coli* expressing the G29D mutant did not degrade RB19 in the medium (Fig. S6).

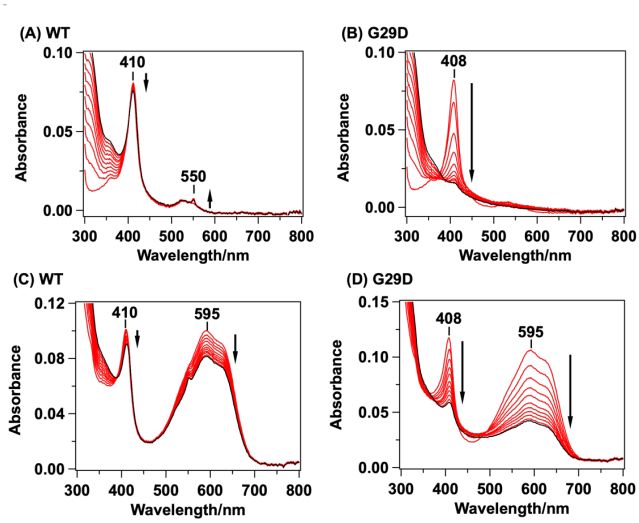

Fig. 10. Stopped-flow kinetic analysis. UV–vis absorption spectral changes upon mixing (A) WT and (B) the G29D mutant (1.0 μM) with H_2O_2 (10 mM); (C) WT and (D) G29D (1.0 μM) with RB19 (40 μM) in the presence of H_2O_2 (10 mM) in sodium phosphate buffer (50 mM, pH 7.0) at 25 °C. Spectra were measured at 6 s intervals for 60 s.

To investigate the reason for the ineffectiveness of the G29D mutant as a whole-cell catalyst, transient kinetic spectral changes were monitored using a stopped-flow apparatus to observe the formation of compound I. The absorption spectra of WT cyt *c* in the absence of RB19 were not affected by the reaction with H_2O_2 except for the appearance of a small peak at 550 nm, which would be derived from the formation of ferrous heme (Fig. 10A). In contrast, the Soret band of the G29D mutant rapidly decreased (Fig. 10B), indicating that heme was broken by H_2O_2. The absence of absorption at 650–690 nm, characteristic of verdoheme, a well-known intermediate in most heme-degradation reactions,[43] suggests that heme was broken by coupled oxidation. The same reaction was monitored in the presence of RB19. Compared with the spectral changes of WT cyt *c*, the absorbance of RB19 (~595 nm) was largely decreased by the G29D mutant (Fig. 10C, D). At the same time, the Soret band of the mutant also rapidly decreased. These results indicate that the dye degradation activity of the G29D mutant is much greater than that of WT cyt *c* (Fig. 10A, B). However, this mutant is not effective as a whole-cell catalyst because heme is easily broken in the reaction with H_2O_2.

Conclusions

In summary, we designed several cyt *c* mutants to confer dye-decolorizing activity. The dye-degrading activity of WT cyt *c* at pH 7.0 was ~60% of that of *Vc*DyP at pH 4.5. To enhance the activity, we replaced Met80 with Ala or Val, but the activity was increased by only ~1.5-fold. To further improve substrate binding affinity we introduced Trp at position 76. The catalytic efficiency (k_{cat}/K_m) of the mutant was ~3-fold greater than that of WT cyt *c*. Finally, to form a hydrogen bond to axial His we replaced Gly29 with Asp. This mutation resulted in a drastic enhancement (~80-fold) of dye-decolorizing activity. Despite this, the mutant did not work well as a whole-cell catalyst due to heme degradation in the reaction with H_2O_2. However, these results from a series of mutations indicate that it is possible to design artificial enzymes that can degrade dyes.

Experimental Procedures

Materials

All chemicals were purchased from Wako Pure Chemical Industries (Osaka, Japan), Nacalai Tesque (Kyoto, Japan), Kanto Chemical (Tokyo, Japan) or Sigma–Aldrich (St. Louis, USA) and used without further purification.

Protein expression and preparation

Escherichia coli strain Rosetta 2(DE3)pLysS cells were transformed with plasmids containing horse heart cyt *c* and yeast cyt *c* heme lyase.[44,45] They were inoculated in 5 mL of Luria-Bertani (LB) medium and grown overnight. This precultured medium was added to 2 L of 2×TY medium supplemented with 100 μg L^{-1} ampicillin and 34 μg L^{-1} chloramphenicol, and the bacteria were further incubated at 37 °C. The expression of cyt *c* was initiated by adding 1 mM isopropyl β-D-thiogalactopyranoside (IPTG) to the culture when the cell density reached an optical density at 600 nm (OD_{600}) of 0.6. Then, 0.1 mM δ-aminolaevulinic acid was added to promote heme biosynthesis. After incubation at 25 °C for an additional 24 h, the cells were collected with centrifugation.

The cell pellet was resuspended in 50 mM Tris-HCl, pH 7.5, containing 1 mg mL^{-1} lysozyme, 50 mg L^{-1} DNase I and RNase A and suspended for 1 h to lyse the cell pellets completely. The supernatant of the crude extract was obtained with centrifugation at 18,000 rpm for 5 min. Ammonium sulfate was added to the supernatant to a concentration of 351 g L^{-1} while stirring at 4 °C. Following centrifugation the supernatant was dialyzed (Spectra/Por, 6,000–8,000 M_r cutoff) overnight in 4 L of buffer A (50 mM sodium phosphate, pH 7.4) to remove ammonium sulfate. The sample was loaded onto a HiTrap SP HP column (Cytiva) with a linear gradient of 1–300 mM NaCl. The eluate sample was concentrated with Amicon ultrafiltration using 3-kDa cutoff membranes. Because purified cyt *c* was a mixture of ferric and ferrous forms, it was oxidized with potassium ferricyanide and further purified using a gel-filtration column (HiLoad 16/60 Superdex 200 pg, Cytiva) equilibrated with 50 mM Tris-HCl and 150 mM NaCl (pH 8.0).

Site-directed mutagenesis

Mutagenesis was conducted utilizing the PrimeSTAR Mutagenesis Basal Kit from Takara Bio (Otsu, Japan) using the WT expression vector as the template. DNA oligonucleotides were purchased from Eurofins Genomics (Tokyo, Japan). The primers used for the construction of mutants are listed in Table S1. Genes were sequenced (Eurofins Genomics) to ensure that only the desired mutations were introduced.

Dye-decolorizing assay

The dye-decolorizing activity was determined by spectrophotometrically measuring the rate of H_2O_2-mediated decomposition of RB19. Briefly, 1.9 mL of protein solution (final concentration of 1 μM) in 50 mM sodium phosphate (pH 7.0) was placed in a 2 mL cuvette along with 10–50 μL of the substrate solution to be tested. The reaction was started by the addition of 3.3 μL of 12 M H_2O_2 (final concentration of 20 mM) in the same buffer, with incubations normally for 5 min at room temperature. The decomposition of the substrate was measured at 595 nm (ε_{595} = 10 mM^{-1} cm^{-1}) using a JASCO V-550 spectrophotometer. H_2O_2 concentrations were determined spectrophotometrically using an absorption coefficient at 240 nm of 43.6 M^{-1} cm^{-1}.[46] The curve of initial rates (v) versus H_2O_2 concentrations was fitted to the Michaelis–Menten equation:

$$v/[\text{protein}] = k_{cat}[H_2O_2]/(K_m + [H_2O_2]) \quad (1)$$

where k_{cat} and K_m are the maximum rate and Michaelis–Menten constant, respectively. The curve of initial rates versus RB19 concentrations was better fitted to the Hill equation:

$$v/[\text{protein}] = k_{cat}[RB19]^h/\{(K_d)^h + [RB19]^h\} \quad (2)$$

where h and K_d are the Hill constant and apparent dissociation constant, respectively.

The turnover rate of the dye-decolorizing activity was calculated by measuring the decrease in absorbance at 595 nm 100 s after initiating the reaction and reported in min^{-1}.

Peroxidase assay

The peroxidase assay was measured spectrophotometrically. The standard assay was performed in 2 mL of the reaction mixture with the enzyme, 10 mM H_2O_2, and an appropriate amount of guaiacol (5–150 μM) at 25 °C. The concentrations of the proteins were 0.1 μM (M80A, M80V, G29D) or 1 μM (WT and P76W) guaiacol. The reaction was initiated with the addition of H_2O_2 and the initial rate for guaiacol oxidation was monitored at 470 nm (ε_{470} = 22.6 mM^{-1} cm^{-1}). Data were fitted to the Michaelis–Menten equation. The rapid reaction of cyt *c* with H_2O_2 was monitored with a stopped-flow apparatus (MSP-1000-V; Unisoku, Osaka, Japan).

Author Contributions

I. O. designed the experiments, conducted experiments, analyzed results and wrote the paper. T.U. coordinated the study, designed the experiments and wrote the paper. K.I. oversaw the project and wrote the paper. All authors read and approved the manuscript.

Conflicts of interest

The authors declare that there are no competing interests associated with the manuscript.

Acknowledgements

This research was supported by JSPS KAKENHI Grant Number JP16K05835, JP20K05700 (T.U.) and JP19H05769 (K.I.).

References

1 S. J. Kim and M. Shoda, *Biotechnol. Bioeng.*, 1999, **62**, 114–119.

2 T. Uchida, M. Sasaki, Y. Tanaka and K. Ishimori, *Biochemistry*, 2015, **54**, 6610–6621.

3 E. Strittmatter, C. Liers, R. Ullrich, S. Wachter, M. Hofrichter, D. A. Plattner and K. Piontek, *J. Biol. Chem.*, 2013, **288**, 4095–4102.

4 D. Linde, R. Pogni, M. Cañellas, F. Lucas, V. Guallar, M. C. Baratto, A. Sinicropi, V. Sáez-Jiménez, C. Coscolín, A. Romero, F. J. Medrano, F. J. Ruiz-Dueñ;as and A. T. Martínez, *Biochem. J.*, 2015, **466**, 253–262.

5 R. Shrestha, X. Chen, K. X. Ramyar, Z. Hayati, E. A. Carlson, S. H. Bossmann, L. Song, B. V. Geisbrecht and P. Li, *ACS Catal.*, 2016, **6**, 8036–8047.

6 M. Zámocký, S. Hofbauer, I. Schaffner, B. Gasselhuber, A. Nicolussi, M. Soudi, K. F. Pirker, P. G. Furtmüller and C. Obinger, *Arch. Biochem. Biophys.*, 2015, **574**, 108–119.

7 P. G. Furtmüller, M. Zederbauer, W. Jantschko, J. Helm, M. Bogner, C. Jakopitsch and C. Obinger, *Arch. Biochem. Biophys.*, 2006, **445**, 199–213.

8 Y. Sugano, R. Muramatsu, A. Ichiyanagi, T. Sato and M. Shoda, *J. Biol. Chem.*, 2007, **282**, 36652–36658.

9 M. Lučić, D. A. Svistunenko, M. T. Wilson, A. K. Chaplin, B. Davy, A. Ebrahim, D. Axford, T. Tosha, H. Sugimoto, S. Owada, F. S. N. Dworkowski, I. Tews, R. L. Owen, M. A. Hough and J. A. R. Worrall, *Angew. Chemie - Int. Ed.*, 2020, **59**, 21656–21662.

10 M. Lučić, A. K. Chaplin, T. Moreno-Chicano, F. S. N. Dworkowski, M. T. Wilson, D. A. Svistunenko, M. A. Hough and J. A. R. Worrall, *Dalton Trans.*, 2020, **49**, 1620–1636.

11 M. N. El-Nahass, M. M. El-keiy and E. M. M. Ali, *Int. J. Biol. Macromol.*, 2018, **116**, 1304–1309.

12 M. Shakeri and M. Shoda, *J. Mol. Catal. B Enzym.*, 2008, **54**, 42–49.

13 M. Shakeri and M. Shoda, *J. Mol. Catal. B Enzym.*, 2010, **62**, 277–281.

14 C. Chen, R. Shrestha, K. Jia, P. F. Gao, B. V. Geisbrecht, S. H. Bossmann, J. Shi and P. Li, *J. Biol. Chem.*, 2015, **290**, 23447–23463.

15 T. Uchida, I. Omura, S. Umetsu and K. Ishimori, *J. Inorg. Biochem.*, 2021, **219**, 111422.

16 Robert A. Scott and A. Grant Mauk, *Third World Plann. Rev.*, 1997, **19**, 117.

17 N. A. Belikova, Y. A. Vladimirov, A. N. Osipov, A. A. Kapralov, V. A. Tyurin, M. V. Potapovich, L. V. Basova, J. Peterson, I. V. Kurnikov and V. E. Kagan, *Biochemistry*, 2006, **45**, 4998–5009.

18 F. Sinibaldi, L. Fiorucci, A. Patriarca, R. Lauceri, T. Ferri, M. Coletta and R. Santucci, *Biochemistry*, 2008, **47**, 6928–6935.

19 P. Zhang, J. Xu, X. J. Wang, B. He, S. Q. Gao and Y. W. Lin, *ACS Catal.*, 2019, **9**, 7888–7893.

20 S. F. Chen, X. C. Liu, J. K. Xu, L. Li, J. J. Lang, G. B. Wen and Y. W. Lin, *Inorg. Chem.*, 2021, **60**, 2839–2845.

21 D. J. Yan, W. Li, Y. Xiang, G. B. Wen, Y. W. Lin and X. Tan, *ChemBioChem*, 2015, **16**, 47–50.

22 L. Le Li, H. Yuan, F. Liao, B. He, S. Q. Gao, G. B. Wen, X. Tan and Y. W. Lin, *Dalton. Trans.*, 2017, **46**, 11230–11238.

23 V. Pfanzagl, K. Nys, M. Bellei, H. Michlits, G. Mlynek, G. Battistuzzi, K. Djinovic-Carugo, S. Van Doorslaer, P. G. Furtmüller, S. Hofbauer and C. Obinger, *J. Biol. Chem.*, 2018, **293**, 14823–14838.

24 D. B. Goodin and D. E. McRee, *Biochemistry*, 1993, **32**, 3313–3324.

25 Z. H. Wang, Y. W. Lin, F. I. Rosell, F. Y. Ni, H. J. Lu, P. Y. Yang, X. S. Tan, X. Y. Li, Z. X. Huang and A. G. Mauk, *ChemBioChem*, 2007, **8**, 607–609.

26 M. Cervelli, P. Mariottini, G. Smulevich, M. Coletta and L. Fiorucci, *J. Inorg. Biochem.*, 2017, **169**, 86–96.

27 M. I. Savenkova, J. M. Kuo and P. R. Ortiz de Montellano, *Biochemistry*, 1998, **37**, 10828–10836.

28 A. K. Chaplin, M. T. Wilson and J. A. R. Worrall, *Dalton Trans.*, 2017, **46**, 9420–9429.

29 G. W. Bushnell, G. V. Louie and G. D. Brayer, *J. Mol. Biol.*, 1990, **214**, 585–595.

30 L. Hannibal, F. Tomasina, D. A. Capdevila, V. Demicheli, V. Tórtora, D. Alvarez-Paggi, R. Jemmerson, D. H. Murgida and R. Radi, *Biochemistry*, 2016, **55**, 407–428.

31 F. Sinibaldi, B. D. Howes, M. C. Piro, P. Caroppi, G. Mei, F. Ascoli, G. Smulevich and R. Santucci, *J. Biol. Inorg. Chem.*, 2006, **11**, 52–62.

32 E. Torres, J. Victor Sandoval, F. I. Rosell, A. Grant Mauk and R. Vazquez-Duhalt, *Enzyme Microb. Technol.*, 1995, **17**, 1014–1020.

33 S. P. Rafferty, M. Smith and A. G. Mauk, *Inorganica Chim. Acta*, 1996, **242**, 171–177.

34 H. Lei, S. M. Nold, L. J. Motta and B. E. Bowler, *Biochemistry*, 2019, **58**, 2921–2933.

35 S. Samsri, P. Prasertsuk, B. Nutho and S. Pornsuwan, *Arch. Biochem. Biophys.*, 2022, **716**, 109112.

36 O. M. Deacon, A. I. Karsisiotis, T. Moreno-Chicano, M. A. Hough, C. MacDonald, T. M. A. Blumenschein, M. T. Wilson, G. R. Moore and J. A. R. Worrall, *Biochemistry*, 2017, **56**, 6111–6124.

37 O. M. Deacon, R. W. White, G. R. Moore, M. T. Wilson and J. A. R. Worrall, *J. Inorg. Biochem.*, 2020, **203**, 110924.

38 A. I. Karsisiotis, O. M. Deacon, M. T. Wilson, C. MacDonald, T. M. A. Blumenschein, G. R. Moore and J. A. R. Worrall, *Sci. Rep.*, 2016, **6**, 1–12.

39 B. C. Finzel, T. L. Poulos and J. Kraut, *J. Biol. Chem.*, 1984, **259**, 13027–13036.

40 A. Guerra-Castellano, I. Díaz-Moreno, A. Velázquez-Campoy, M. A. De La Rosa and A. Díaz-Quintana, *Biochim. Biophys. Acta - Bioenerg.*, 2016, **1857**, 387–395.

41 G. Mahapatra, A. Varughese, Q. Ji, I. Lee, J. Liu, A. Vaishnav, C. Sinkler, A. A. Kapralov, C. T. Moraes, T. H. Sanderson, T. L. Stemmler, L. I. Grossman, V. E. Kagan, J. S. Brunzelle, A. R. Salomon, B. F. P. Edwards and M. Hüttemann, *J. Biol. Chem.*, 2017, **292**, 64–79.

42 G. E. Arnold, L. A. Day and A. Keith Dunker, *Biochemistry*, 1992, **31**, 7948–7956.

43 T. Uchida, Y. Sekine, T. Matsui, M. Ikeda-Saito and K. Ishimori, *Chem. Commun.*, 2012, **48**, 6741–6743.

44 W. B. R. Pollock, F. I. Rosell, M. B. Twitchett, M. E. Dumont and A. G. Mauk, *Biochemistry*, 1998, **37**, 6124–6131.

45 W.-Y. Jeng, C.-Y. Chen, H.-C. Chang and W.-J. Chuang, *J. Bioenerg. Biomembr.*, 2002, **34**, 423–431.

46 R. F. Beers and I. W. Sizer, *J. Biol. Chem.*, 1952, **195**, 133–140.